Int. J. Heat Mass Transfer. Vol. 36, No. 2, pp. 383–389, 1993
Printed in Great Britain

0017-9310/93 $6.00+0.00

Thermal dispersion and inertia effects on vortex instability of a horizontal mixed convection flow in a saturated porous medium

JIIN-YUH JANG and JIING-LIN CHEN
Department of Mechanical Engineering, National Cheng-Kung University, Tainan, Taiwan 70101, R.O.C.

(*Received* 7 *January* 1992 *and in final form* 16 *March* 1992)

Abstract—A numerical analysis is made to analyze the thermal dispersion and inertia effects on the vortex mode of instability of a horizontal mixed convection boundary layer flow with a uniform free stream velocity in a saturated porous medium adjacent to a uniform heat flux surface. The stability analysis is based on the linear stability theory and the resulting eigenvalue problem is solved by the local similarity method. The critical Rayleigh number and the associated wave number at the onset of vortex instability are obtained for various values of thermal dispersion and inertia parameters. It is found that the thermal dispersion effect stabilizes the flow to the vortex mode of disturbance, while the inertia effect destabilizes it.

1. INTRODUCTION

THE PROBLEMS of the vortex mode of instability in natural or mixed convection flow over a heated plate in a saturated porous medium have recently received considerable attention. This is primarily due to a large number of technical applications, such as fluid flow in geothermal reservoirs, separation processes in chemical industries, storage of radioactive nuclear waste materials, transpiration cooling, transport processes in aquifers, etc. The instability mechanism is due to the presence of a buoyancy free component in the direction normal to the plate surface.

For natural convection boundary layer flow adjacent to a flat plate, Hsu *et al.* [1] and Hsu and Cheng [2] analyzed the vortex mode of instability of horizontal and inclined natural convection flows in a porous medium. Jang and Chang [3] re-examined the same problem for an inclined plate, where both the streamwise and normal components of the buoyancy force are retained in the momentum equations. Jang and Chang [4] studied the vortex instability of horizontal natural convection in a porous medium resulting from combined heat and mass buoyancy effects. The effects of a density extremum on the vortex instability of an inclined buoyant layer in porous media saturated with cold water were examined by Jang and Chang [5, 6].

For mixed convection boundary layer flow adjacent to a flat plate, Hsu and Cheng [7] analyzed the vortex instability for horizontal mixed convection in a porous medium. By neglecting the normal component of buoyancy force, Cheng [8] showed that, in the main flow analysis, the mixed convection boundary layer flow over an inclined plate in a saturated porous medium can be approximated by the similarity solution for a vertical plate, with the gravity component parallel to the inclined plate incorporated in the Rayleigh number. Following the same approach, Hsu and Cheng [9] applied a linear stability analysis to determine the condition of onset of vortex instability for flow over an inclined surface. It is apparent that the instability results in ref. [9] are not valid for angles of inclination from the horizontal that are small. Thus, Jang and Lie [10] provided new vortex instability results for small angles of inclination from the horizontal ($\phi \leqslant 25^\circ$) and more accurate results for large angles of inclination ($\phi > 25^\circ$) than the previous study [9].

All of the works mentioned above are based on the Darcy formulation. However, at higher flow rates or in a high porosity medium, there is a departure from Darcy's law and the inertia (velocity-squared term), thermal dispersion, convective (development term) and boundary (no-slip condition) effects not included in the Darcy model may become significant. Chang and Jang [11, 12] were the first authors to study the non-Darcy effects (inertia, boundary and convective effects) on the vortex instability of a horizontal natural convection boundary layer flow in a saturated porous medium. One effect which has not been accounted for in refs. [11, 12] is that due to transverse thermal dispersion. It has been shown that the thermal dispersion effect may become very important when the inertial effect is prevalent [13, 14]. The thermal dispersion effect on the vortex instability of a free or mixed convection boundary layer flow in a porous medium, to the authors' knowledge, does not seem to have been investigated. This has motivated the present investigation. It should be noted that a related problem for the onset of convection of the flow in a porous medium bounded by two horizontal impermeable

NOMENCLATURE

A	constant in the wall temperature relation
a	dimensional spanwise wave number
c	inertia parameter
d	mean particle diameter or pore diameter
Er	Ergun number, $c\alpha_0/d\nu$
f	similarity stream function profile
F	dimensionless disturbance stream function amplitude
g	gravitational acceleration
h	local heat transfer coefficient
k	dimensionless wave number
K	permeability
k_0	stagnant conductivity
Nu	local Nusselt number, hx/k_0
p'	perturbation pressure
p	pressure
Pe_x	local Peclet number, $U_\infty x/\alpha_0$
Ra_d	Rayleigh number based on the pore diameter, $Kg\beta A d^{3/2}/\alpha_0\nu$
Ra_x	modified local Rayleigh number, $Kg\beta(T_w-T_\infty)x/\alpha_0\nu$
T	temperature
T'	perturbation temperature
$\tilde{T}$	disturbance temperature amplitude
$\tilde{u}$	x direction disturbance velocity amplitude
u, v, w	volume averaged velocity in the x, y, z directions
u', v', w'	disturbance velocity in the x, y, z directions
x, y, z	axial, normal and spanwise coordinates.

Greek symbols

α_d	thermal diffusivity due to dispersion effect
α_{eff}	effective thermal diffusivity
α_0	stagnant thermal diffusivity
β	coefficient of thermal expansion
γ	dispersion coefficient
η	similarity variable
θ	dimensionless temperature, $(T-T_\infty)/(T_w-T_\infty)$
Θ	dimensionless disturbance temperature amplitude
λ	exponent on wall temperature relation
μ	absolute viscosity
ν	kinematic viscosity
ξ	mixed convection parameter, $Pe_x^{3/2}/Ra_x$
ρ	density
ψ	stream function
ψ'	disturbance stream function
$\tilde{\psi}$	disturbance stream function amplitude.

Subscripts

w	condition at the wall
∞	condition at the free stream.

Superscript

*	critical condition.

plates with an imposed vertical temperature gradient has been the subject of studies by Rubin [15, 16], Neischloss and Dagan [17], Kvernvold and Tyvand [18] and Georgiadis and Catton [19].

The purpose of this paper is to examine the thermal dispersion effect on the vortex instability of a horizontal mixed convection flow in a porous medium. Since both thermal dispersion and inertia are important at high Rayleigh numbers [13], they are included in this study. The boundary effect on the vortex instability has been investigated in our previous paper [12], and is shown to stabilize the flow; this effect is neglected in the present study in order to obtain the similarity solution for the base flow [14]. The analysis of the disturbance flow is based on the linear stability theory. The disturbance quantities are assumed to be in the form of a stationary vortex roll that is periodic in the spanwise direction, with its amplitude function depending primarily on the normal coordinate and weakly on the streamwise coordinate. The resulting eigenvalue problem is solved using a variable step-size sixth-order Runge–Kutta integration scheme in conjunction with the Gram–Schmidt orthogonalization procedure [20] to maintain the linear independence of the eigenfunctions.

2. MATHEMATICAL FORMULATION

2.1. *The base flow*

Consider the problems of steady mixed convection in a semi-infinite porous medium bounded by a horizontal impermeable surface aligned parallel to a free stream with uniform velocity U_∞ and temperature T_∞, where x represents the distance along the plate from its leading edge, and y the distance normal to the surface. The wall temperature is assumed to be a power function of x, i.e. $T_w = T_\infty + Ax^\lambda$, where A and λ are constants. If we assume that: (i) local thermal equilibrium exists between the fluid and solid phases; (ii) the physical properties are considered to be constant, except for the density term that is associated with the body force; and (iii) the Boussinesq approximation is employed, then the governing equations are given by

$$\frac{\partial u}{\partial x}+\frac{\partial v}{\partial y}=0 \tag{1}$$

$$u+\frac{\rho c}{\mu}u^2 = -\frac{K}{\mu}\frac{\partial p}{\partial x} \tag{2}$$

$$v+\frac{\rho c}{\mu}v^2 = -\frac{K}{\mu}\left[\frac{\partial p}{\partial y}-\rho g\beta(T-T_\infty)\right] \tag{3}$$

$$u\frac{\partial T}{\partial x}+v\frac{\partial T}{\partial y}=\frac{\partial}{\partial y}\left(\alpha_{\text{eff}}\frac{\partial T}{\partial y}\right) \tag{4}$$

where K is the permeability of the porous medium, β is the coefficient of thermal expansion, c is the transport property related to the inertia effect, α_{eff} is the effective thermal diffusivity which can be expressed as: $\alpha_{\text{eff}}=\alpha_0+\alpha_d$, where α_0 is the stagnant diffusivity and α_d is the molecular diffusivity due to thermal dispersion. The other symbols are defined in the Nomenclature. Here we adopt the following thermal dispersion model proposed by Plumb [21], that is

$$\alpha_d=\gamma ud \tag{5}$$

where γ is the dispersion coefficient, which has a value ranging from 1/7 to 1/3 and d is the mean particle diameter.

The pressure terms appearing in equations (2) and (3) can be eliminated through cross-differentiation and subtraction. By applying the boundary layer assumptions and introducing the stream function ψ which automatically satisfies equation (1), equations (1)–(4) become

$$\frac{\partial^2\psi}{\partial y^2}+\frac{c}{v}\frac{\partial}{\partial y}\left[\left(\frac{\partial\psi}{\partial y}\right)^2\right]=-\frac{Kg\beta}{v}\frac{\partial T}{\partial x} \tag{6}$$

$$\frac{\partial\psi}{\partial y}\frac{\partial T}{\partial x}-\frac{\partial\psi}{\partial x}\frac{\partial T}{\partial y}=\frac{\partial}{\partial y}\left(\alpha_{\text{eff}}\frac{\partial T}{\partial y}\right). \tag{7}$$

The corresponding boundary conditions are

$$\begin{aligned}
&y=0,\quad v=0,\quad T_w=T_\infty+Ax^\lambda\\
&y\to\infty,\quad T=T_\infty,\quad u=0 \quad \text{for free convection}\\
&\qquad\qquad\qquad\qquad u=u_\infty \quad \text{for mixed convection.}
\end{aligned} \tag{8}$$

Lai and Kulacki [14] have shown that similarity solutions for equations (6)–(8) exist only if $\lambda=0.5$ (i.e. constant heat flux). The suitable similarity variables are as follows:

$$\eta=Ra_x^{1/3}\frac{y}{x},\quad f(\eta)=\frac{\psi}{\alpha_0\,Ra_x^{1/3}},\quad \theta=\frac{T-T_\infty}{T_w-T_\infty}. \tag{9}$$

Then the governing equations for the case flow are

$$f''+Er(Ra_d)^{2/3}[(f')^2]'+\frac{\theta}{2}-\frac{\eta}{2}\theta'=0 \tag{10}$$

$$\tfrac{1}{2}(f'\theta-f\theta')=\theta''+\gamma(Ra_d)^{2/3}(f'\theta''+f''\theta') \tag{11}$$

and the transformed boundary conditions are

$$\begin{aligned}
&\eta=0,\quad \theta=1,\quad f=0\\
&\eta\to\infty,\quad \theta=0,\quad f'=\xi^{2/3}
\end{aligned} \tag{12}$$

where $\xi=Pe_x^{3/2}/Ra_x$, is the mixed convection parameter; $Pe_x=U_\infty x/\alpha_0$, the local Peclet number; $Ra_x=Kg\beta(T_w-T_\infty)x/\alpha_0 v$, the modified local Rayleigh number; $Ra_d=Kg\beta Ad^{2/3}/\alpha_0 v$, the Rayleigh number based on the pore diameter; and $Er=c\alpha_0/dv$, the dimensionless inertia parameter (Ergun number).

It is noted that ξ is the mixed convection parameter, which measures the relative importance of forced to free convection; $\xi=0$ corresponds to the case of purely free convection. γ and Er express the relative importance of thermal dispersion and inertia effects, respectively. As $\gamma=Er=0$, equations (10) and (11) reduce to Darcy's model.

In terms of the dimensionless variables, it can be shown that the local Nusselt number is given by

$$\frac{Nu}{Ra_x^{1/3}}=-[1+\gamma(Ra_d)^{2/3}f'(0)]\theta'(0). \tag{13}$$

2.2. *The disturbance flow*

The standard method of the linear stability theory is that in which the instantaneous values of the velocity, pressure and temperature are perturbed by small amplitude disturbances and the base flow equations are subtracted, with terms higher than first-order in disturbance quantities being neglected. Then we get the following disturbance equations:

$$\frac{\partial u'}{\partial x}+\frac{\partial v'}{\partial y}+\frac{\partial w'}{\partial z}=0 \tag{14}$$

$$u'+\frac{2c}{v}\bar{u}u'=-\frac{K}{\mu}\frac{\partial p'}{\partial x} \tag{15}$$

$$v'+\frac{2c}{v}\bar{v}v'=-\frac{K}{\mu}\left(\frac{\partial p'}{\partial y}-\rho g\beta T'\right) \tag{16}$$

$$w'=-\frac{K}{\mu}\frac{\partial p'}{\partial z} \tag{17}$$

$$\begin{aligned}
&\bar{u}\frac{\partial T'}{\partial x}+\bar{v}\frac{\partial T'}{\partial y}+u'\frac{\partial \bar{T}}{\partial x}+v'\frac{\partial \bar{T}}{\partial y}\\
&\quad=\alpha_0\left(\frac{\partial^2 T'}{\partial x^2}+\frac{\partial^2 T'}{\partial y^2}+\frac{\partial^2 T'}{\partial z^2}\right)\\
&\quad+\gamma d\left(\frac{\partial\bar{u}}{\partial y}\frac{\partial T'}{\partial y}+\bar{u}\frac{\partial^2 T'}{\partial y^2}+\frac{\partial u'}{\partial y}\frac{\partial \bar{T}}{\partial y}+u'\frac{\partial^2\bar{T}}{\partial y^2}+\bar{u}\frac{\partial^2 T'}{\partial z^2}\right)
\end{aligned} \tag{18}$$

where the barred and primed quantities signify the base flow and disturbance components, respectively.

Following the method of order-of-magnitude analysis prescribed in detail by Hsu and Cheng [2], the terms $\partial u'/\partial x$, $\partial^2 T'/\partial x^2$ in equations (14) and (18) can be neglected. The omission of $\partial u'/\partial x$ in equation (14) implies the existence of a disturbance stream function ψ' such that

$$v'=-\frac{\partial\psi'}{\partial z},\quad w'=\frac{\partial\psi'}{\partial y}. \tag{19}$$

We assume that the three-dimensional disturbances are of the form

$$(\psi',u',T')=[\tilde{\psi}(x,y),\tilde{u}(x,y),\tilde{T}(x,y)]\exp(iaz+q(x)) \tag{20}$$

where a is the spanwise periodic wave number, and

$$q(x) = \int \alpha_i(x)\,\mathrm{d}x$$

with $\alpha_i(x)$ denoting the spatial growth factor. For the lowest order approximation $q(x) = \alpha_i x$. Setting $\alpha_i = 0$ for neutral stability yields

$$\mathrm{i}a\tilde{u} + \frac{2\mathrm{i}ac}{\nu}\bar{u}\tilde{u} = \frac{\partial^2\tilde{\psi}}{\partial x\,\partial y} \tag{21}$$

$$\frac{\partial^2\tilde{\psi}}{\partial y^2} - a^2\tilde{\psi} - \frac{2ca^2}{\nu}\bar{v}\tilde{\psi} = -\frac{\mathrm{i}aK\rho g\beta}{\mu}\tilde{T} \tag{22}$$

$$\alpha_0\left[\frac{\partial^2\tilde{T}}{\partial y^2} - a^2\tilde{T}\right] + \gamma d\left[\frac{\partial\bar{u}}{\partial y}\frac{\partial\tilde{T}}{\partial y} + \bar{u}\frac{\partial^2\tilde{T}}{\partial y^2} + \frac{\partial\tilde{u}}{\partial y}\frac{\partial\bar{T}}{\partial y} + \tilde{u}\frac{\partial^2\bar{T}}{\partial y^2} - a^2\bar{u}\tilde{T}\right] = \bar{u}\frac{\partial\tilde{T}}{\partial x} + \bar{v}\frac{\partial\tilde{T}}{\partial y} + \tilde{u}\frac{\partial\bar{T}}{\partial x} - \mathrm{i}a\tilde{\psi}\frac{\partial\bar{T}}{\partial y}. \tag{23}$$

Equations (21)–(23) are solved based on the local similarity approximations [2], wherein the disturbances are assumed to have weak dependence in the streamwise direction (i.e. $\partial/\partial x \ll \partial/\partial\eta$). Introducing the following dimensionless quantities

$$k = \frac{ax}{Ra_x^{1/3}},\quad F(\eta) = \frac{\tilde{\psi}}{\mathrm{i}\alpha_0\,Ra_x^{1/3}},\quad \Theta(\eta) = \frac{\tilde{T}}{T_w - T_\infty} \tag{24}$$

we obtain the following system of equations for the local similarity approximations

$$F'' - (1 - B_4\,Er\,Ra_d^{2/3}\,Ra_x^{-1/3})k^2F = -Ra_x^{1/3}\,k\Theta \tag{25}$$

$$(1 + B_2\gamma\,Ra_d^{2/3})\Theta'' + \left(\frac{B_1}{2} + B_3\gamma\,Ra_d^{2/3}\right)\Theta' - \left(k^2 + \frac{B_2}{2} + \gamma\,Ra_d^{2/3}\,k^2\right)\Theta = \frac{B_7\gamma\,Ra_d^{2/3}\,\eta}{2B_5k\,Ra_x^{1/3}}F''' + \left(\frac{B_8\gamma\,Ra_d^{2/3}}{2B_5k\,Ra_x^{1/3}} - \frac{B_9\gamma\,Ra_d^{4/3}\,Er\,\eta}{B_5^2k\,Ra_x^{1/3}} - \frac{B_{10}\eta}{4B_5k\,Ra_x^{1/3}}\right)F'' + B_7k\,Ra_x^{1/3}\,F \tag{26}$$

with the boundary conditions

$$F(0) = \Theta(0) = F(\infty) = \Theta(\infty) = 0 \tag{27}$$

where the primes indicate the derivatives with respect to η. Equation (27) arises from the fact that the disturbances vanish at the wall and in the free stream in the porous medium. The coefficients $B_1(\eta)$–$B_{10}(\eta)$ in the equations can be expressed as

$$\begin{aligned} B_1 &= f & B_6 &= f'' + \eta f''' \\ B_2 &= f' & B_7 &= \theta' \\ B_3 &= f'' & B_8 &= \theta' + \eta\theta'' \\ B_4 &= f - \eta f' & B_9 &= \theta' f'' \\ B_5 &= 1 + 2Er\,Ra_d^{2/3}f' & B_{10} &= \theta - \eta\theta'. \end{aligned} \tag{28}$$

Substitution of equation (25) into equation (26) leads to

$$\begin{aligned} &F'''' + A_0\left(\frac{B_1}{2} + B_3\gamma\,Ra_d^{2/3} + \frac{B_7\gamma\,Ra_d^{2/3}\,\eta}{2B_5}\right)F''' \\ &+ A_0\left[\frac{2B_8\gamma\,Ra_d^{2/3} - B_{10}\eta}{4B_5} - \frac{B_9\gamma\,Ra_d^{4/3}\,Er\,\eta}{B_5^2} - (1 + B_2\gamma\,Ra_d^{2/3})(k^2 - B_4B_0) - (1 + \gamma\,Ra_d^{2/3})k^2 - \frac{B_2}{2}\right]F'' \\ &- A_0\left[2(1 + B_2\gamma\,Ra_d^{2/3})B_3B_0\eta + \left(\frac{B_1}{2} + B_3\gamma\,Ra_d^{2/3}\right)(k^2 - B_4B_0)\right]F' \\ &+ A_0\left[\left(k^2 + \frac{B_2}{2} + \gamma\,Ra_d^{2/3}\,k^2\right)(k^2 - B_4B_0) + B_7k^2\,Ra_x^{2/3} - (1 + B_2\gamma\,Ra_d^{2/3})B_6B_0 - \left(\frac{B_1}{2} + B_3\gamma\,Ra_d^{2/3}\right)B_3B_0\eta\right]F = 0 \end{aligned} \tag{29}$$

with boundary conditions

$$F(0) = F''(0) = F(\infty) = F''(\infty) = 0 \tag{30}$$

where

$$A_0 = \frac{1}{(1 + B_2\gamma\,Ra_d^{2/3})},\quad B_0 = Er\,Ra_d^{2/3}\,Ra_x^{-1/3}\,k^2.$$

Equations (29) and (30) constitute a fourth-order system of linear ordinary differential equations for the disturbance amplitude distribution $F(\eta)$. For fixed Ra_d, ξ, γ and Er, the solution F is an eigenfunction for the eigenvalues Ra_x and k.

3. NUMERICAL METHOD OF SOLUTION

In the stability calculations, the disturbance equations are solved by separately integrating two linearly independent integrals. The full solution may be written as the sum of two linearly independent solutions $F(\eta) = F_1(\eta) + EF_2(\eta)$. The two independent integrals $F_1(\eta)$ and $F_2(\eta)$ may be chosen so that their asymptotic solutions are

$$F_1(\eta_\infty) = N\exp(\Gamma\eta_\infty),\quad F_2(\eta_\infty) = \exp(\Lambda\eta_\infty) \tag{31}$$

where

$$N = -\frac{Ra_x^{1/3}\,k}{\Gamma^2 - \Lambda^2}$$

$$\Gamma = -\frac{1}{2}\left\{\frac{B_1/2}{1+B_2\gamma\,Ra_d^{2/3}} + \left[\left(\frac{B_1/2}{1+B_2\gamma\,Ra_d^{2/3}}\right)^2 + \frac{4(k^2+B_2/2+\gamma\,Ra_d^{2/3}\,k^2)}{1+B_2\gamma\,Ra_d^{2/3}}\right]^{1/2}\right\}$$

$$\Lambda = -(1-B_4\,Er\,Ra_d^{2/3}\,Ra_x^{-1/3})^{1/2}k.$$

A sixth-order variable step size Runge–Kutta integration routine is used here to solve first the base flow system, equations (10) and (11), and the results are stored for a fixed step size, $\Delta\eta = 0.02$, which is small enough to predict accurate linear interpolation between mesh points. Equation (29) with boundary conditions, equation (30), is then solved as follows. For specified Ra_d, ξ, γ, Er and k, Ra_x is estimated. Using equation (31) as starting values, the two integrals are integrated separately from the outer edge of the boundary layer to the wall using a sixth-order Runge–Kutta variable step size integrating routine incorporated with the Gram–Schmidt orthogonalization procedure [20] to maintain the linear independence of the eigenfunctions. The required input of the base flow to the disturbance equations is calculated, as necessary, by linear interpolation of the stored base flow. From the values of the integrals at the wall, E is determined using the boundary condition $F(0) = 0$. A Taylor series expansion of the second boundary condition $F''(0) = 0$ provides a correction scheme for the initial estimate of Ra_x. Iterations continue until the second boundary condition is sufficiently close to zero ($< 10^{-6}$, typically).

4. RESULTS AND DISCUSSION

Numerical results for the tangential velocity, temperature profiles, Nusselt number, neutral stability curves, the critical Rayleigh number and wave number at the onset of vortex instability are presented for various values of thermal dispersion coefficient γ and inertia parameter Er with mixed convection parameter ξ ranging from 0 to 10 and with $Ra_d = 20$.

Figures 1 and 2 show simultaneously the velocity and temperature profiles across the boundary layer for the selected values of γ (0, 0.15 and 0.3) and Er (0 and 0.05) for $\xi = 0$ (purely free convection) and 1, respectively. The velocity profiles are referred to the left and lower axes, while the temperature profiles are referred to the right and upper axes. The dashed lines denote the results when the inertia effect is completely neglected ($Er = 0$). It should be noted that Darcy's law [1, 7] corresponds to the case of $\gamma = Er = 0$. It is seen that both the thermal dispersion and inertia effects markedly affect the velocity and temperature profiles. We observe that the velocity increases with increasing values of the thermal dispersion coefficient γ. As the inertia effect is considered ($Er \neq 0$), the magnitude of velocity near the wall decreases. These imply that thermal dispersion tends to enhance the heat transfer, while the inertia effect tends to reduce the heat transfer. Figure 3 shows the alteration of Nusselt number with γ for various values of mixed convection parameter ξ and for $Er = 0.05$ and 0. It is seen that, as would be expected, the thermal dispersion effect increases the heat transfer rate, while the inertia effect decreases it.

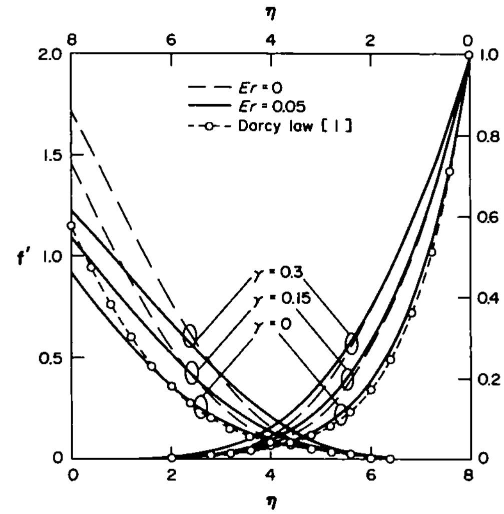

FIG. 1. Tangential velocity and temperature profiles across the boundary layer for selected values of γ and Er for $\xi = 0$ (purely free convection).

Figures 4 and 5 show the neutral stability curves, in terms of the Rayleigh number Ra_x and the dimensionless wave number k for selected values of γ (0, 0.15 and 0.3) for $\xi = 0$ (purely free convection) and 1, respectively. It is observed that as γ increases, the neutral stability curves shift to a higher Rayleigh number and a lower wave number, indicating a stabilization of the flow to the vortex instability. The neutral stability curves that were obtained by neglecting the inertia effect ($Er = 0$) are plotted with dashed

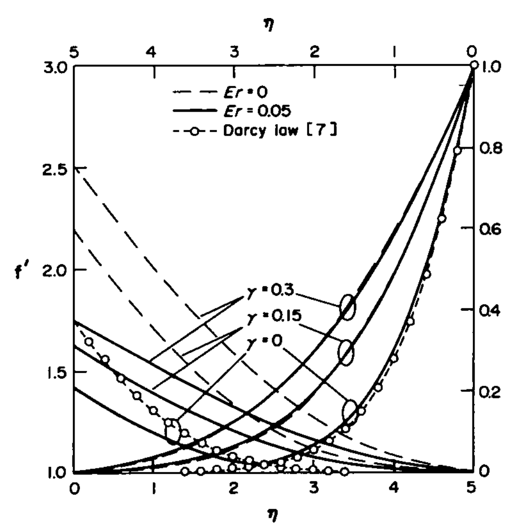

FIG. 2. Tangential velocity and temperature profiles across the boundary layer for selected values of γ and Er for $\xi = 1$ (mixed convection).

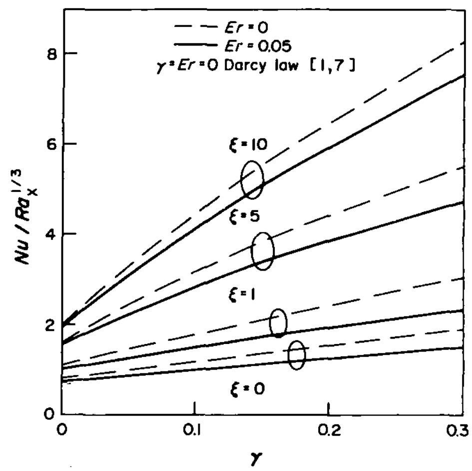

Fig. 3. Alteration of $Nu/Ra_x^{1/3}$ with γ for various values of ξ.

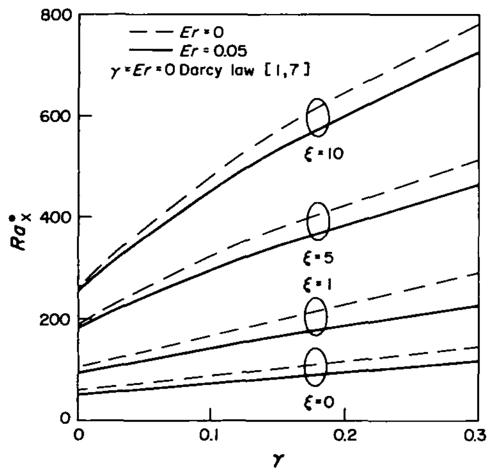

Fig. 6. Critical Rayleigh number as a function of γ for various values of ξ.

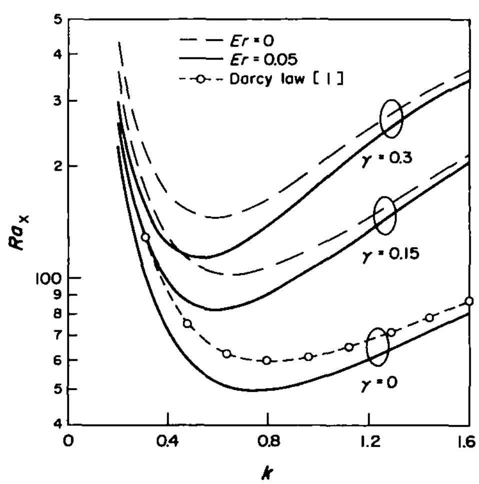

Fig. 4. Neutral stability curves for various values of γ for $\xi = 0$ (purely free convection).

lines in the figures for comparison. It is seen that when the inertia effect is considered, the neutral stability curves shift to a lower Rayleigh number and a lower wave number, indicating a destabilization of the flow.

The critical Rayleigh number Ra_x^* and wave number k^*, which mark the onset of longitudinal vortices, can be found from the minima of the neutral stability curves. The critical Rayleigh number and wave number are plotted as functions of dispersion coefficient γ in Figs. 6 and 7, respectively. Dashed lines represent the case of $Er = 0$, in which the inertia effect is completely neglected. Note that the case of Darcy's law ($\gamma = Er = 0$) for a horizontal surface was considered by Hsu *et al.* [1] for natural convection and by Hsu and Cheng [7] for mixed convection. For $\gamma = Er = 0$, the present results are in good agreement with those of refs. [1, 7]. The numerical values of Ra_x^* and k^* for selected values of ξ, γ and Er are also listed in Table 1 for future reference. The results indicate that the thermal dispersion effect tends to stabilize the flow, while the inertia effect tends to destabilize it. It is

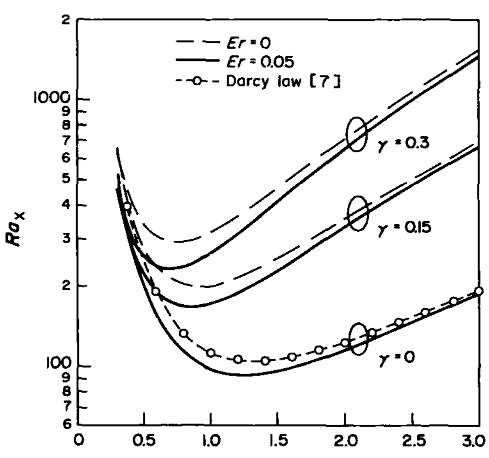

Fig. 5. Neutral stability curves for various values of γ for $\xi = 1$ (mixed convection).

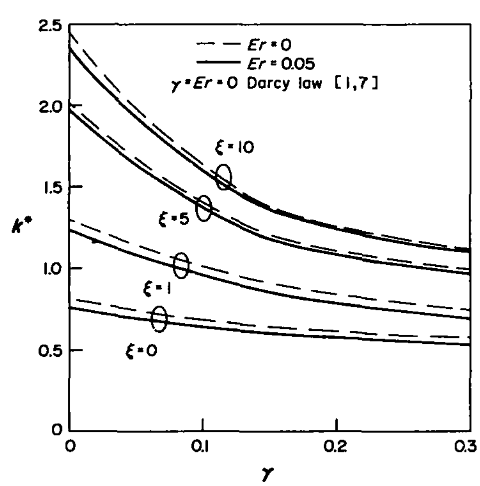

Fig. 7. Critical wave number as a function of γ for various values of ξ.

Table 1. The critical Rayleigh and wave number for selected values of ξ, γ and Er with $Ra_d = 20$

		Ra_x^*		k^*	
ξ	γ	$Er = 0.05$	$Er = 0$	$Er = 0.05$	$Er = 0$
0	0	50.21	59.57	0.7529	0.8065
	0.15	84.31	101.82	0.5994	0.6408
	0.3	118.34	145.81	0.5341	0.5750
1	0	92.72	104.35	1.2415	1.3000
	0.15	165.89	198.04	0.8497	0.9069
	0.3	226.42	290.16	0.6901	0.7450
5	0	181.33	190.74	1.9777	2.0308
	0.15	344.79	378.30	1.1750	1.2070
	0.3	464.98	514.60	0.9645	0.9942
10	0	253.00	260.00	2.3500	2.4497
	0.15	534.45	572.26	1.3596	1.3836
	0.3	725.65	782.77	1.1000	1.1204

interesting to note that the variation of the critical Rayleigh number Ra_x^* vs the thermal dispersion coefficient γ exhibits an almost linear function. It is also seen that the critical Rayleigh number Ra_x^* is a strong function of the mixed convection parameter ξ. The larger the values of ξ, the more stable is the flow for the vortex instability. It is apparent from Fig. 7 that when either γ or Er increases, the critical wave number k^* decreases. A close look at Figs. 6 and 7 indicates that the thermal dispersion effect is more pronounced as the mixed convection parameter ξ increases. For $\xi = 0$ (natural convection), the deviation of the critical Rayleigh number from that for Darcy flow is about 41.5% for $\gamma = 0.15$, while for $\xi = 10$ (mixed convection), the deviation is up to 105.6% for $\gamma = 0.15$.

5. CONCLUSIONS

The thermal dispersion and inertia effects on the vortex instability of horizontal mixed convection boundary layer flow in a saturated porous medium have been examined by a linear stability theory. The numerical results demonstrate that the thermal dispersion effect enhances the heat transfer rate and stabilizes the flow, while for the inertia effect the opposite trend is true. It is shown that the thermal dispersion effect is more pronounced as the mixed convection parameter ξ increases. Moreover, it is found that the flow is less susceptible to the vortex instability for higher values of mixed convection parameter ξ and thus aided mixed convection ($\xi > 0$) is more stable than free convection ($\xi = 0$).

REFERENCES

1. C. T. Hsu, P. Cheng and G. M. Homsy, Instability of free convection flow over a horizontal impermeable surface in a porous medium, *Int. J. Heat Mass Transfer* **21,** 1221–1228 (1978).
2. C. T. Hsu and P. Cheng, Vortex instability in buoyancy-induced flow over inclined heated surfaces in porous media, *J. Heat Transfer* **101,** 660–665 (1979).
3. J. Y. Jang and W. J. Chang, Vortex instability of buoyancy-induced inclined boundary layer flow in a saturated porous medium, *Int. J. Heat Mass Transfer* **31,** 759–767 (1988).
4. J. Y. Jang and W. J. Chang, The flow and vortex instability of horizontal natural convection in a porous medium resulting from combined heat and mass buoyancy effects, *Int. J. Heat Mass Transfer* **31,** 769–777 (1988).
5. J. Y. Jang and W. J. Chang, Vortex instability of inclined buoyancy layer in porous media saturated with cold water, *Int. Commun. Heat Mass Transfer* **14,** 405–416 (1987).
6. J. Y. Jang and W. J. Chang, Maximum density effects on vortex instability of horizontal and inclined buoyancy induced flows in porous media, *J. Heat Transfer* **111,** 572–574 (1989).
7. C. T. Hsu and P. Cheng, Vortex instability of mixed convective flow in a semi-infinite porous medium bounded by a horizontal surface, *Int. J. Heat Mass Transfer* **23,** 789–798 (1980).
8. P. Cheng, Combined free and forced convection flow about inclined surfaces in porous media, *Int. J. Heat Mass Transfer* **20,** 807–814 (1977).
9. C. T. Hsu and P. Cheng, The onset of longitudinal vortices in mixed convective flow over an inclined surface in a porous medium, *J. Heat Transfer* **102,** 544–549 (1980).
10. J.-Y. Jang and K.-N. Lie, Vortex instability of mixed convection flow over horizontal and inclined surfaces in a porous medium, *Int. J. Heat Mass Transfer* **35,** 2077–2085 (1992).
11. W. J. Chang and J. Y. Jang, Inertia effects on vortex instability of a horizontal natural convection flow in a saturated porous medium, *Int. J. Heat Mass Transfer* **32,** 541–550 (1989).
12. W. J. Chang and J. Y. Jang, Non-Darcian effects on vortex instability of a horizontal natural convection flow in a porous medium, *Int. J. Heat Mass Transfer* **32,** 529–539 (1989).
13. J. T. Hong, Y. Yamada and C. L. Tien, Effects of non-Darcian and nonuniform porosity on vertical plate natural convection in porous media, *J. Heat Transfer* **109,** 356–362 (1987).
14. F. C. Lai and F. A. Kulacki, Thermal dispersion effect on non-Darcy convection over horizontal surfaces in saturated porous media, *Int. J. Heat Mass Transfer* **32,** 971–976 (1989).
15. H. Rubin, Heat dispersion effect on thermal convection in a porous medium layer, *J. Hydrol.* **21,** 173–185 (1974).
16. H. Rubin, A note on the heat dispersion effect on thermal convection in a porous medium layer, *J. Hydrol.* **25,** 167–168 (1975).
17. H. Neischloss and G. Dagan, Convective currents in a porous layer heated from below: the influence of hydrodynamic dispersion, *Physics Fluids* **18,** 757–761 (1975).
18. O. Kvernvold and P. A. Tyvand, Dispersion effects on thermal convection in porous media, *J. Fluid Mech.* **99,** 673–686 (1980).
19. J. G. Georgiadis and I. Catton, Dispersion in cellular thermal convection in porous layers, *Int. J. Heat Mass Transfer* **31,** 1081–1091 (1988).
20. A. R. Wazzan, T. T. Okamura and H. M. O. Smith, Stability of laminar boundary layers at separation, *Physics Fluids* **10,** 2540–2545 (1967).
21. O. A. Plumb, The effect of thermal dispersion on heat transfer in packed bed boundary layers, *Proc. 1st ASME/JSME Thermal Engng Joint Conf.*, Vol. 2, pp. 17–21. *ASME*, Tokyo (1983).